

# On-site approximation for spin-orbit coupling in LCAO density functional methods

Lucas Fernández-Seivane,<sup>1</sup> Miguel A. Oliveira,<sup>2,\*</sup> Stefano Sanvito,<sup>2</sup> Jaime Ferrer<sup>1</sup>

<sup>1</sup> *Departamento de Física, Universidad de Oviedo, 33007 Oviedo, Spain and*

<sup>2</sup> *Department of Physics, Trinity College, Dublin 2, Ireland\**

(Dated: December 2, 2024)

We propose a computational method that simplifies drastically the inclusion of spin-orbit interaction in density functional theory implemented on localised atomic orbital basis sets. Our method is based on a well-known procedure for obtaining pseudopotentials from atomic relativistic *ab initio* calculations and on an on-site approximation for the spin-orbit matrix elements. We have implemented the technique in the SIESTA<sup>1</sup> code, and we show that it provides accurate results for the overall band structure and splittings of group IV and III-IV semiconductors as well as for 5d metals.

## I. INTRODUCTION

Computational methods in condensed matter physics are a powerful tool for predicting and explaining the most diverse properties of materials, nanostructures, mesoscopic structures and small biological systems. Among an enormous plethora of methodologies, density functional theory (DFT)<sup>2,3</sup> has become a standard for simulations in the atomic and nanometric length scale. Several numerical implementations of DFT are available where the details of the algorithm usually depend on the specific applications the method is designed for. These implementations can be divided broadly into two large categories according to the basis functions used: plane-waves or linear combination of atomic orbitals (LCAO). The first are typically easier to implement and have as a clear advantage the fact that convergence is determined by a single variational parameter, usually the the energy cut-off. In contrast the second are based on a tight binding description of the chemical bond, they are usually more cumbersome to implement and the variational principle is controlled by the set of parameters defining the basis functions. However these second methods are ideal for linear scaling since sparse Hamiltonian can be constructed by using strictly confined orbitals.

Recently, the growing interest in the field of spintronics,<sup>4</sup> has generated the need for the inclusion of the spin-orbit interaction in the description of the electronic structure. Spin-orbit coupling determines the finite spin-relaxation time of electrons in ordinary semiconductors and in semiconductor heterostructures,<sup>5</sup> and also some aspects of the physics of diluted magnetic semiconductors.<sup>6</sup> These systems pose a serious challenge to computational methods since large unit cells are needed for a correct description of heterojunctions and diluted materials. Spin-orbit coupling, together with magnetic dipolar interactions, also give rise to the magnetic anisotropies that determine the direction of the magnetisation vector in spintronics devices, specially in reduced dimensions.<sup>7</sup>

Usually, the spin-orbit interaction is expected to make small, though noticeable, contributions to the electronic structure and total energy of materials and devices composed of atoms with small atomic number. For instance,

the magnetic anisotropy energies of the cubic phases of Fe, Co and Ni is of the order of a few  $\mu\text{eV}$  per atom and therefore only highly accurate implementations of DFT are able to reproduce them.<sup>8</sup> The spin-orbit strength will however increase with atomic number and becomes large for 5d transition metals and heavy semiconductors.

We have developed a general method to include the spin-orbit interaction in conventional pseudopotential based LCAO DFT methods, that is not computationally demanding and is therefore fully adequate for large scale simulations. The method, although not suitable for highly accurate total energy calculations, provides an excellent description of the effects of spin-orbit coupling on the electronic structure. We have also implemented the method in the LCAO program SIESTA,<sup>1</sup> but we wish to stress that the method is general and it could have been implemented in any other pseudopotential code based on localized wave-functions that can handle non-collinear arrangements of electron spin.<sup>9,10</sup> We present in this article the details of the method and our numerical implementation (section II) as well as the excellent results obtained in our tests of group IV and III-IV semiconductors and of 5d metals (sections III and IV, respectively).

## II. THE ON-SITE APPROXIMATION

### A. Relativistic effects in pseudopotential methods

Kleinman and Bylander have shown that the procedures for generation of non-relativistic pseudopotentials can easily be extended to account for relativistic effects.<sup>11,12</sup> The procedure relies on solving self-consistently the all-electrons Dirac equation of a single atom first. The pseudopotentials thus computed  $V_j$ , that depend now on the total angular momentum  $j = l \pm \frac{1}{2}$ , are extracted. The pseudopotential Hamiltonian can therefore be written as

$$\hat{V} = \sum_{j, m_j} |j, m_j\rangle V_j \langle j, m_j|, \quad (1)$$

and includes all relativistic corrections to order  $\alpha^2$  where  $\alpha$  is the fine structure constant and  $|j, m_j\rangle$  are total angular momentum states.

This expression can be recast in a form suitable for non-relativistic pseudopotential theory by expressing  $|j, m_j\rangle$  in terms of a tensor product of the regular angular momentum states  $|l, m\rangle$  and the eigenstates of the  $z$  component of the Pauli spin matrices<sup>13</sup>

$$\begin{aligned} |j = l + \frac{1}{2}, m_j\rangle &= \begin{pmatrix} \sqrt{\frac{l+m_j+\frac{1}{2}}{2l+1}} |l, m_j - \frac{1}{2}\rangle \\ \sqrt{\frac{l-m_j+\frac{1}{2}}{2l+1}} |l, m_j + \frac{1}{2}\rangle \end{pmatrix}, \\ |j = l - \frac{1}{2}, m_j\rangle &= \begin{pmatrix} \sqrt{\frac{l-m_j+\frac{1}{2}}{2l+1}} |l, m_j - \frac{1}{2}\rangle \\ -\sqrt{\frac{l+m_j+\frac{1}{2}}{2l+1}} |l, m_j + \frac{1}{2}\rangle \end{pmatrix}. \end{aligned} \quad (2)$$

Equation (1) can then be rewritten<sup>14</sup> as

$$\begin{aligned} \hat{\mathbf{V}} &= \hat{\mathbf{V}}^{sc} + \hat{\mathbf{V}}^{SO} = \\ &= \sum_{l,m} [\bar{V}_l \mathbb{1}_\sigma + \bar{V}_l^{SO} \vec{L} \cdot \vec{\mathbf{S}}] |l, m\rangle \langle l, m|, \end{aligned} \quad (3)$$

where we use bold letters to indicate 2x2 matrices, with  $\mathbb{1}_\sigma$  representing the unit operator in spin space,

$$\vec{L} \cdot \vec{\mathbf{S}} = \frac{1}{2} \begin{pmatrix} \hat{L}_z & \hat{L}_- \\ \hat{L}_+ & -\hat{L}_z \end{pmatrix}, \quad (4)$$

and,

$$\begin{aligned} \bar{V}_l &= \frac{1}{2l+1} [(l+1)V_{l+\frac{1}{2}} + lV_{l-\frac{1}{2}}], \\ \bar{V}_l^{SO} &= \frac{2}{2l+1} [V_{l+\frac{1}{2}} - V_{l-\frac{1}{2}}]. \end{aligned} \quad (5)$$

It should be stressed that the scalar part  $\hat{\mathbf{V}}^{sc}$  of the pseudopotential contains now not only the conventional non-relativistic pseudopotential, but also the scalar relativistic corrections.

The vectors  $|l, m\rangle$ , representing complex spherical harmonics, form a complete basis for the Hilbert space of the angular momentum operator  $\vec{L}$ . It is a useful practice in solid state physics and quantum chemistry to replace them with real spherical harmonics  $|l, M\rangle$ , since the corresponding Hamiltonian is a real matrix. The change of basis is achieved by the following unitary transformation

$$\begin{aligned} |l, M\rangle &= \frac{1}{\sqrt{2}} (|l, m\rangle + (-1)^m |l, \bar{m}\rangle), \\ |l, \bar{M}\rangle &= \frac{1}{\sqrt{2}i} (|l, m\rangle - (-1)^m |l, \bar{m}\rangle), \end{aligned} \quad (6)$$

which is valid for  $M > 0$  ( $\bar{M} = -M$ ,  $\bar{m} = -m$ ). The case  $M = 0$  is simply given by  $|l, M = 0\rangle = |l, m = 0\rangle$ .

The pseudopotential operator  $\hat{\mathbf{V}}$  of equation (3), is now written as

$$\begin{aligned} \hat{\mathbf{V}} &= \hat{\mathbf{V}}^{sc} + \hat{\mathbf{V}}^{SO} = \\ &= \sum_{l,M} [\bar{V}_l \mathbb{1}_\sigma + \bar{V}_l^{SO} \vec{L} \cdot \vec{\mathbf{S}}] |l, M\rangle \langle l, M|. \end{aligned} \quad (7)$$

Finally the Kohn-Sham Hamiltonian<sup>3</sup> is expressed as a sum of kinetic energy  $\hat{\mathbf{T}}$ , scalar relativistic  $\hat{\mathbf{V}}^{sc}$ , spin-orbit  $\hat{\mathbf{V}}^{SO}$ , Hartree  $\hat{\mathbf{V}}^H$  and exchange and correlation  $\hat{\mathbf{V}}^{xc}$  potentials

$$\hat{\mathbf{H}} = \hat{\mathbf{T}} + \hat{\mathbf{V}}^{sc} + \hat{\mathbf{V}}^{SO} + \hat{\mathbf{V}}^H + \hat{\mathbf{V}}^{xc}. \quad (8)$$

This Hamiltonian is therefore a  $2 \times 2$  matrix in spin space

$$\hat{\mathbf{H}} = \begin{bmatrix} \hat{H}^{\uparrow\uparrow} & \hat{H}^{\uparrow\downarrow} \\ \hat{H}^{\downarrow\uparrow} & \hat{H}^{\downarrow\downarrow} \end{bmatrix}, \quad (9)$$

whose non-diagonal blocks arise from the spin-orbit part and from the exchange and correlation potential, whenever the system under consideration displays a non-collinear spin.<sup>9,10</sup>

### B. Spin-orbit in LCAO methods: on-site approximation to the Hamiltonian matrix elements

LCAO methods expand the eigenstates  $|\psi_n\rangle$  of the non-collinear Kohn-Sham Hamiltonian over a set of localised orbitals  $|\phi_i\rangle$ ,

$$|\psi_n\rangle = \sum_i \begin{pmatrix} c_{n,i}^\uparrow \\ c_{n,i}^\downarrow \end{pmatrix} |\phi_i\rangle \quad (10)$$

where  $i$  is a collective index for all the symbols required to describe uniquely a given orbital

$$|\phi_i\rangle = |\phi_{n_i, l_i, M_i}\rangle = |R_{n_i, l_i}\rangle \otimes |l_i, M_i\rangle \quad (11)$$

where both radial and angular parts of the wave function  $\phi_i(\vec{r} - \vec{d}_i) = \langle \vec{r} | \phi_i \rangle$  are centered at the position  $\vec{d}_i$ . Here  $n_i$  does not necessarily describe the principle quantum number only, it generally labels a set of radial functions associated to the angular momentum  $l_i$  according to the multiple zetas scheme.<sup>15</sup>

The Kohn-Sham equation,  $\hat{H} |\psi_n\rangle = E_n |\psi_n\rangle$ , is then projected onto such orbital basis set as

$$\begin{bmatrix} H_{ij}^{\uparrow\uparrow} - E_n S_{ij} & H_{ij}^{\uparrow\downarrow} \\ H_{ij}^{\downarrow\uparrow} & H_{ij}^{\downarrow\downarrow} - E_n S_{ij} \end{bmatrix} \begin{bmatrix} c_{n,j}^\uparrow \\ c_{n,j}^\downarrow \end{bmatrix} = 0, \quad (12)$$

where  $H_{ij}^{\sigma\sigma'} = \langle \phi_i | \hat{H}^{\sigma\sigma'} | \phi_j \rangle$  and  $S_{ij} = \langle \phi_i | \phi_j \rangle$  are the matrix elements of the Hamiltonian and overlap matrix respectively.

The spin-orbit term can then be calculated as

$$\begin{aligned} \mathbf{V}_{ij}^{SO} &= \langle \phi_i | \hat{\mathbf{V}}^{SO} | \phi_j \rangle = \\ &= \sum_{k, l_k, M_k} \langle \phi_i | \bar{V}_{l_k}^{SO} \vec{L} \cdot \vec{\mathbf{S}} | l_k, M_k \rangle \langle l_k, M_k | \phi_j \rangle, \end{aligned} \quad (13)$$

where index  $k$  indicates the atom on which the potential is centered,  $\bar{V}_{l_k}^{SO} = \bar{V}_l^{SO}(\vec{r} - \vec{d}_k)$ , and  $|l_k, M_k\rangle$  is the spherical harmonic centered at the same atomic position  $\vec{d}_k$ .

Equation (13) involves a considerable number of three-center integrals. Inclusion of the spin-orbit interaction is therefore, in the LCAO approach, if straightforward, computationally intensive. One possibility of reducing the computational effort is to construct fully non-local pseudopotentials.<sup>16</sup> We note however that the radial part of the spin-orbit pseudopotentials,  $\bar{V}_l^{SO}$ , is very short-ranged, resulting in matrix elements that decay quickly

with the distance among the three centers. Thus we consider only matrix elements where the three components, both orbitals and the pseudopotential, reside on the same atom, and discard all the rest. This approximation simplifies the matrix elements of equation (13) to one center integrals, and drastically reduces the computational effort needed to account for spin-orbit effects. We obtain accordingly

$$\begin{aligned} \mathbf{V}_{ij}^{SO} &= \frac{1}{2} \sum_{k, l_k > 0, M_k} \langle R_{n_i, l_i} | \bar{V}_{l_k}^{SO} | R_{n_j, l_j} \rangle \langle l_i, M_i | \begin{pmatrix} \hat{L}_z & \hat{L}_- \\ \hat{L}_+ & -\hat{L}_z \end{pmatrix} | l_k, M_k \rangle \langle l_k, M_k | l_j, M_j \rangle \\ &\approx \frac{1}{2} \langle R_{n_i, l_i} | \bar{V}_{l_i}^{SO} | R_{n_j, l_i} \rangle \langle l_i, M_i | \begin{pmatrix} \hat{L}_z & \hat{L}_- \\ \hat{L}_+ & -\hat{L}_z \end{pmatrix} | l_i, M_j \rangle \delta_{l_i, l_j}, \end{aligned} \quad (14)$$

since the  $\hat{L}_\alpha$  operators leave each  $l_i$  subspace invariant. The angular part of these on-site matrix elements can be calculated analytically

$$\begin{aligned} \langle l_i, M_i | \hat{L}_z | l_i, M_j \rangle &= i M_j \delta_{M_i, \overline{M_j}}, \\ \langle l_i, M_i | \hat{L}_\pm | l_i, 0 \rangle &= \pm \frac{A_0^\pm}{\sqrt{2}} (\delta_{M_i, 1} \pm i \delta_{M_i, \overline{1}}), \\ \langle l_i, M_i | \hat{L}_\pm | l_i, M_j \rangle &= \frac{1}{2} \left\{ A_{M_j}^+ \left( \delta_{M_i, M_j+1} \pm i \delta_{M_i, \overline{M_j+1}} \right) - A_{M_j}^- \left( \delta_{M_i, M_j-1} \mp i \delta_{M_i, \overline{M_j-1}} \right) \right\}, \\ \langle l_i, M_i | \hat{L}_\pm | l_i, \overline{M_j} \rangle &= \frac{1}{2} \left\{ A_{M_j}^+ \left( \delta_{M_i, M_j+1} \pm i \delta_{M_i, \overline{M_j+1}} \right) + A_{M_j}^- \left( \delta_{M_i, M_j-1, M'} \mp i \delta_{M_i, \overline{M_j+1}} \right) \right\}, \end{aligned} \quad (15)$$

where  $A_{M_j}^\pm = \sqrt{l_i(l_i+1) - M_j(M_j \pm 1)}$  are Clebsch-Gordan coefficients.

Some useful symmetries of the matrix elements of the Hamiltonian and of its spin-orbit part should also be highlighted. Since the Hamiltonian is hermitian the matrix elements satisfy the relationship

$$H_{ij}^{\sigma\sigma'} = (H_{ji}^{\sigma'\sigma})^*. \quad (16)$$

It is also easy to show that all terms in the Hamiltonian satisfy a spin box hermiticity, *i.e.*

$$H_{ij}^{\sigma\sigma'} = (H_{ij}^{\sigma'\sigma})^*, \quad (17)$$

except the spin-orbit contribution which is spin box anti-hermitian

$$H_{ij}^{\sigma\sigma'} = -(H_{ij}^{\sigma'\sigma})^*. \quad (18)$$

This property has important consequences for the calculation of the total energy.

### C. Density matrix and total energy

The  $2 \times 2$  charge density matrix can be written in terms of the LCAO basis as

$$\begin{aligned} \mathbf{n}(\vec{r}) &= \sum_n f_n \psi_n(\vec{r}) \psi_n(\vec{r})^\dagger = \\ &= \sum_{i,j} \phi_i(\vec{r} - \vec{d}_i) \phi_j^*(\vec{r} - \vec{d}_j) \rho_{ij} \end{aligned} \quad (19)$$

where  $f_n$  represents the occupation of the Kohn-Sham eigenstate  $\psi_n(\vec{r})$  and  $\rho_{ij}$  is a  $2 \times 2$  matrix containing the products of wave-function coefficients, whose components are

$$\rho_{ij}^{\sigma\sigma'} = \sum_n f_n c_{n,i}^\sigma c_{n,j}^{\sigma'}. \quad (20)$$

The electronic contribution to the total energy may be expressed as a sum of a band-structure (BS) contribution plus double-counting corrections. The BS contribution can be written in the LCAO basis as

$$E_e^{BS} = \sum_n f_n \langle \psi_n | \hat{\mathbf{H}} | \psi_n \rangle = \sum_{i,j,\sigma,\sigma'} H_{ij}^{\sigma\sigma'} \rho_{ji}^{\sigma'\sigma}, \quad (21)$$

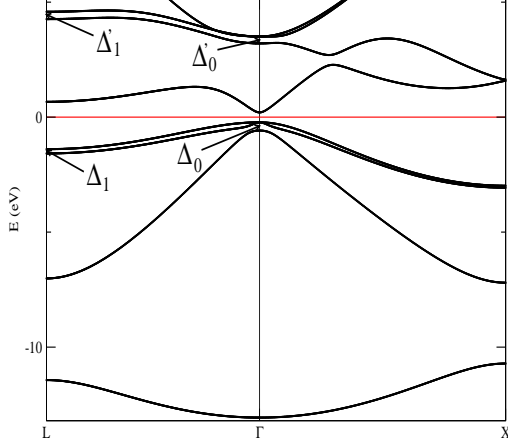


FIG. 1: Band structure of GaAs calculated with our on-site implementation of the spin-orbit interaction.

which may also be expressed as

$$\sum_{ij} \left\{ H_{ij}^{\uparrow\uparrow} \rho_{ji}^{\uparrow\uparrow} + H_{ij}^{\downarrow\downarrow} \rho_{ji}^{\downarrow\downarrow} + 2 \operatorname{Re} \left[ (V_{ij}^{xc\uparrow\downarrow} - V_{ij}^{SO\uparrow\downarrow}) (\rho_{ji}^{\uparrow\downarrow})^* \right] \right\} \quad (22)$$

where we have isolated the non-diagonal contributions in spin space, which arise only from the spin-orbit interaction and from the exchange and correlation potential, whenever spin non-collinearity is present. The spin-orbit contribution to the total energy is

$$E^{SO} = \operatorname{Tr} \sum_{i,j} \mathbf{V}_{ij}^{SO} \rho_{ji}, \quad (23)$$

since there are no double-counting terms.

#### D. Forces and stresses

One important consequence of the on-site approximation is that spin-orbit does not give rise to an explicit contribution to forces and stresses, even though an implicit contribution due to the modification of the self-consistent wave-function is always present. According to the Hellmann-Feynman theorem,<sup>17</sup> the spin-orbit contribution to the forces exerted upon an atom centered at position  $\vec{d}_k$  is obtained by simply differentiating the energy with respect to the atomic coordinates of the atom,

$$\begin{aligned} -\vec{F}_k^{SO} &= \vec{\nabla}_k E^{SO} = \\ &= \operatorname{Tr} \sum_{i,j} \left\{ \left[ \vec{\nabla}_k \hat{V}_{ij}^{SO} \right] \rho_{ji} + \mathbf{V}_{ij}^{SO} \left[ \vec{\nabla}_k \hat{\rho}_{ji} \right] \right\}, \quad (24) \end{aligned}$$

Basis	$E_T$ (eV)	$\Delta_0$ (eV)	$\Delta'_0$ (eV)	$\Delta_1$ (eV)	$\Delta'_1$ (eV)
SZ	-214.8	0.051	0.025	-	-
DZ	-215.0	0.068	0.157	0.027	0.105
TZ	-215.2	0.068	0.002	0.023	0.078
SZP	-215.8	0.042	0.787	0.024	0.032
DZP	-216.0	0.044	0.647	0.024	0.047
TZP	-216.0	0.045	0.696	0.025	0.050
TZDP	-216.0	0.045	0.604	0.026	0.043
TZTP	-216.0	0.045	0.593	0.026	0.044
TZTPF	-216.1	0.044	0.615	0.025	0.030
REF	-	0.044	0.04	0.02	0.03

TABLE I: Spin-orbit energy splittings of bulk Si calculated for increasingly complete basis sets.  $E_T$  is the total energy,  $\Delta_0$ ,  $\Delta'_0$ ,  $\Delta_1$  and  $\Delta'_1$  are the splittings as defined in the text. REF corresponds to the reference values, experimental whenever possible, as described in the literature.<sup>18</sup>

where both the  $i$  and  $j$  orbitals are centered at the same atomic position  $\vec{d}_k$  and  $\vec{\nabla}_k = \vec{\nabla}_{\vec{d}_k}$ . However both contributions to the spin-orbit forces in equation (24) vanish. The first one is identically zero since the one-center integrals do not depend on the atomic position,

$$\nabla_k \langle R_{n_i, l_i} | \bar{V}_{l_k}^{SO} | R_{n_j, l_j} \rangle \equiv 0. \quad (25)$$

The second term may be rewritten as

$$-\sum_{ij} \left( \mathcal{E}_{ij}^{SO, \uparrow\uparrow} + \mathcal{E}_{ij}^{SO, \downarrow\downarrow} \right) \vec{\nabla}_k S_{ji}, \quad (26)$$

where  $\mathcal{E}_{ij}^{SO, \sigma\sigma'}$  are the components of the spin-orbit contribution to the energy-density matrix

$$\mathcal{E}_{ij}^{SO} = \frac{1}{2} \sum_{l,m} (S_{il}^{-1} \mathbf{V}_{lm}^{SO} \rho_{mj} + \rho_{il} \mathbf{V}_{lm}^{SO} S_{mj}^{-1}). \quad (27)$$

However, since  $\mathcal{E}^{SO}$  is antisymmetric with respect to the orbital indices, in contrast to the overlap matrix that is symmetric, the second term vanishes as well.

In a similar way one can demonstrate that the spin-orbit interaction in the on-site approximation does not introduce any additional contribution to the stress.

### III. SPIN-ORBIT IN GROUP IV AND III-V SEMICONDUCTORS

We have thus demonstrated that in general our on-site approximation simplifies the inclusion of spin-orbit effects in LCAO DFT codes. We have implemented the method in SIESTA, a LCAO code able to simulate non-collinear arrangements of spins,<sup>1,10</sup> that in addition reads relativistically generated pseudopotentials in the form required by equation (1).

Basis	$a$ (Å)	$BM$ (GPa)	$E_c$ (eV)
DZP	5.392	98.2	5.480
TZP	5.389	98.8	5.485
TZTP	5.388	98.2	5.491
PW	5.384	95.9	5.369
LAPW	5.41	96	5.28
EXP	5.43	98.8	4.64

TABLE II: Structural parameters of bulk Si for several basis sets.  $a$  is the lattice parameter,  $BM$  the bulk modulus and  $E_c$  the cohesive energy. PW refers to a 50 Ryd cutoff plane-wave calculation.<sup>1</sup> LAPW corresponds to an all-electrons linear-augmented-plane-wave calculation<sup>22</sup> and EXP to the experimental values.<sup>23</sup>

The numerical implementation is rather simple since the spin-orbit contribution to the Hamiltonian does not depend on the electron charge density and therefore does not need to be updated during the self-consistent procedure. This drastically reduces the computational overheads, which are almost identical to those of a standard non-collinear spin-polarised calculation. Here we present a series of test cases for the band-structures of group IV and III-V semiconductors, obtained with the local spin density approximation and norm-conserving relativistic pseudopotentials. Special care was taken in the generation of the pseudopotentials and of the basis sets and in the choice of the parameters that control the numerical accuracy of real and reciprocal space integrals.<sup>1</sup> In particular the basis set was highly optimised following the scheme proposed in references [19,20], from which we have borrowed our notation for multiple zeta basis sets SZ, SZP, DZ, DZP, TZ, TZP, TZDP, TZTP, TZTPF.

The introduction of the spin-orbit interaction lifts specific degeneracies in the band-structure of a material. In particular, for diamond and zincblende semiconductors the six fold degenerate valence band  $\Gamma_{15}^v$ , at  $\Gamma$  splits in two. The first is four-fold degenerate  $\Gamma_8^v$  (the heavy and light hole bands), and the second is only two fold degenerate  $\Gamma_7^v$  (the spin-split-off band). This energy splitting  $\Delta_0$  ( $\Gamma_{15}^v \rightarrow \Gamma_8^v, \Gamma_7^v$ ), is the hallmark of the effects of spin-orbit interaction in the band-structure of these materials. Other commonly measured energy splittings are called  $\Delta'_0$  ( $\Gamma_{15}^c \rightarrow \Gamma_8^c, \Gamma_7^c$ ),  $\Delta_1$  ( $L_3^v \rightarrow L_{4,5}^v, L_6^v$ ) and  $\Delta'_1$  ( $L_3^c \rightarrow L_{4,5}^c, L_6^c$ ).

We show in Fig. 1 the band-structure of the canonical III-V semiconductor, GaAs. The figure also defines graphically the energy splittings described in the previous paragraph. We note first that the band-structure closely resembles that obtained with other methodologies, and also agrees rather well with the experimental data,<sup>18</sup> except for the characteristic LDA underestimation of the semiconductor gap, which is further reduced because of the spin-orbit energy splitting. Therefore, in all the tests that follow, we have avoided narrow gap semiconductors, which are usually predicted to be metals by LDA.<sup>21</sup>

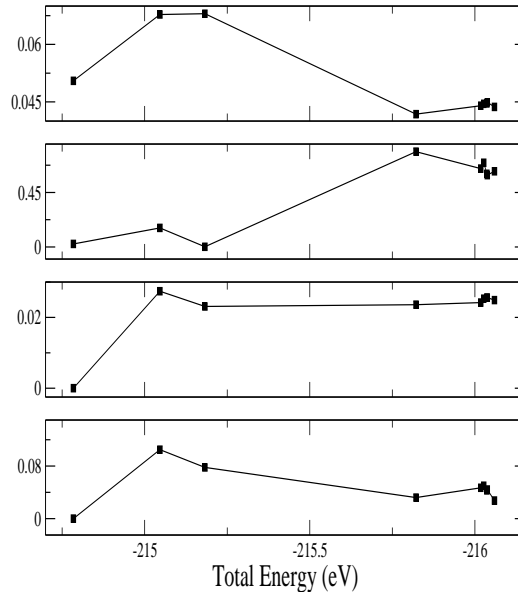


FIG. 2: Convergence of the spin-orbit energy splittings of bulk Si with the size of the basis set. From top to bottom panels, we present respectively  $\Delta_0$ ,  $\Delta'_0$ ,  $\Delta_1$  and  $\Delta'_1$  as functions of the total energy associated with each set. The points correspond to SZ, DZ, TZ, SZP, DZP, TZP, TZDP, TZTP and TZTPF, respectively.

### A. Band structure of Si

The spin-orbit energy splittings of silicon at the high symmetry points of the diamond lattice are presented in Table I and Fig. 2 for increasingly complete basis sets. Our results are in extremely good agreement with

Material	$\Delta_0$ (eV)	$\Delta'_0$ (eV)	$\Delta_1$ (eV)	$\Delta'_1$ (eV)
Ge	0.2959	0.3783	0.1545	0.356
REF <sup>24</sup>	0.287	0.200	0.184	0.266
GaAs	0.3573	0.3006	0.1857	0.319
REF <sup>18</sup>	0.34	0.26	0.23	0.11
AlAs	0.3073	0.0762	0.1636	0.118
REF <sup>25</sup>	0.28	0.04	0.20	-
AlSb	0.6847	0.1752	0.3440	0.307
REF <sup>18</sup>	0.75	0.1	0.4	0.09

TABLE III: Spin splittings for several III-V semiconductors as calculated with a DZP basis set. REF correspond to reference values, experimental whenever possible, as described in the literature.<sup>18,24,25</sup>

the theoretical and experimental data available in the literature.<sup>18</sup> We note that a DZP basis set, which is usually assumed to be the minimal basis needed to obtain reasonably converged results, already provides accurate predictions for the energy splittings. The  $\Delta'_0$  split is somehow an anomaly, and in general we find that the splittings of the conduction bands are not as well described as those of the valence bands. We note that Kohn-Sham eigenvalues should not be associated to single particle excitation energies, since the former are simply the Lagrangian multipliers leading to the Kohn-Sham equations. This is valid for both the valence and the conduction bands. However it is commonly accepted that DFT band structures are a good first approximation to single particle energies of occupied states. The conduction bands are somehow different since such states do not contribute to either the total energy and the density matrix, and therefore are irrelevant in DFT. For this reason a stark disagreement in the conduction band splitting should not be surprising. Moreover, the systematic overestimation of the  $\Delta'_0$  splitting is related to the underestimation of the bandgap. This produces an erroneous enhancement of the hybridisation between the orbitals forming the conduction bands with those forming the valence one, with a net overestimation of the spin-orbit splitting. It is therefore expected that corrective schemes to the bandgap may also correct the spin-orbit splitting of the conduction bands.

Finally we have calculated the Si bulk parameters for different basis sets in order to check that the inclusion of spin-orbit interaction does not change significantly the LDA results. A summary of all the computed structural parameters is presented in Table II.

### B. III-V semiconductors

We have further tested our method by calculating the various energy splittings of Ge, GaAs, AlAs and AlSb, that are group IV and III-V semiconductors with a reasonable gap size. We have again found that DZP basis sets provide essentially converged results. Table III shows that the splittings calculated with a DZP basis agree rather well with other theoretical estimates and with experimental values, with the expected exception of  $\Delta'_0$ . We note that the other theoretical methods are much more computationally demanding.

## IV. 5d METALS: Au AND Pt

Since the spin-orbit interaction is a relativistic effect, it is expected to increase with the atomic number. Therefore, metals from the fifth row of the periodic table are an ideal test ground for our method. Among those, gold and platinum are specially good candidates, since the first is a closed- $d$  shell noble metal while the  $d$ -bands of the second have considerable weight at the Fermi energy.

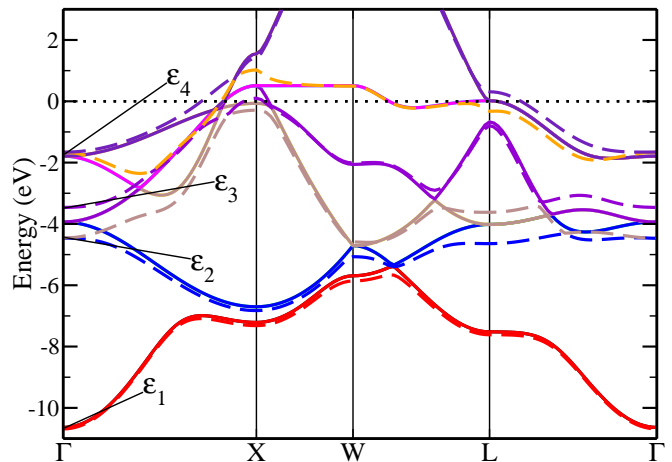


FIG. 3: Band-structure of platinum obtained at the theoretical equilibrium lattice constant. The dashed line is for a spin-orbit calculation, while the solid line is obtained when the spin-orbit coupling is not included. The figure also provides a graphical definition of the energies at the  $\Gamma$  point,  $\epsilon_i$ , of the bands that are closest to the Fermi energy.

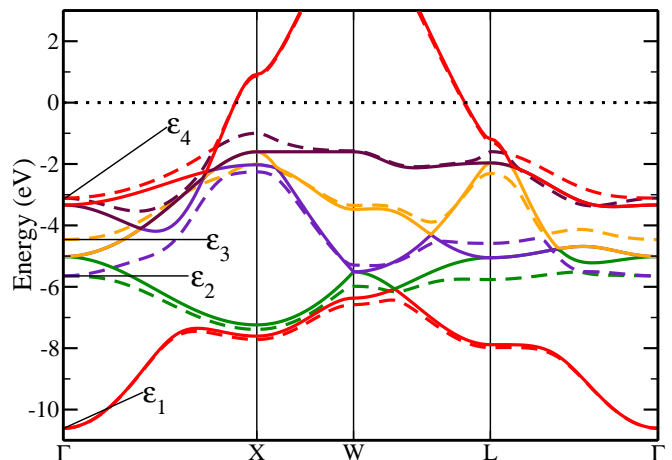


FIG. 4: Band structure of gold obtained at the equilibrium theoretical lattice constant. The dashed line is for a spin-orbit calculation, while the solid line is obtained when the spin-orbit coupling is not included. The figure also provides a graphical definition of the energies at the  $\Gamma$  point,  $\epsilon_i$ , of the bands that are closest to the Fermi energy.

Moreover, a number of *ab initio* spin-orbit calculations are available<sup>26</sup> which demonstrate that the spin-orbit interaction is essential for the correct description of their band structures. To simulate these two materials, we have again used the LDA approximation for exchange and correlation potential, and constructed an optimised set consisting of two atomic wave functions in each of the s-, p- and d-channels.

In Figs. 3 and 4 we present the band-structures of Pt and Au, calculated at the theoretical lattice constant,

Pt	SIESTA+On-site	PWSCF	KKR	APW
$a_0$ (Bohr)	7.45	7.40	7.36	7.414
$\varepsilon_1$ (eV)	-10.53	-10.45	-10.56	-10.35
$\varepsilon_2$ (eV)	-4.38	-4.38	-4.48	-4.24
$\varepsilon_3$ (eV)	-3.38	-3.39	-3.47	-3.28
$\varepsilon_4$ (eV)	-1.62	-1.53	-1.65	-1.48
Au	SIESTA+On-site	PWSCF	KKR	APW
$a_0$ (Bohr)	7.61	7.64	7.637	7.638
$\varepsilon_1$ (eV)	-10.613	-10.18	-10.23	-9.95
$\varepsilon_2$ (eV)	-5.645	-5.43	-5.41	-5.32
$\varepsilon_3$ (eV)	-4.460	-4.23	-4.23	-4.14
$\varepsilon_4$ (eV)	-3.111	-2.97	3.04	2.96

TABLE IV: Lattice constant and energy  $\varepsilon_i$  of selected bands at  $\Gamma$  point obtained with the use of the approximation presented in this article (SIESTA+On-site), and with PWSCF<sup>26</sup>, KKR<sup>27</sup> and APW<sup>28</sup> methods. The definition of the energies  $\varepsilon_i$  is provided in Figs. (3) and (4).

with and without taking into account the spin-orbit coupling. the figures show that s-bands are not modified by spin-orbit, while p- and d-bands suffer strong modifications, specially whenever two bands cross each other. Moreover, we find that the spin-orbit interaction lifts degeneracies at the band crossings as expected.

We summarise in Table IV the bulk lattice constant and the energy of some selected bands at the  $\Gamma$  point, that we define graphically in Fig. 3. These energies are in good agreement with other much more expensive methods, like Plane-wave pseudopotential (PWSCF)<sup>26</sup> and relativistic full-potential Korringa-Kohn-Rostoker (KKR)<sup>27</sup> methods or augmented plane-wave (APW) approaches for solving Dirac equation.<sup>28</sup> We note that the differences range in the order of only a few per cent.

## V. CONCLUSION

We have presented a simple and effective method for including the spin-orbit interaction in standard LCAO

DFT calculations, which is based on relativistic norm-conserving pseudopotentials and on an on-site approximation to the spin-orbit matrix elements. The method is computational undemanding and extremely simple to implement in standard LCAO DFT codes, such as SIESTA. Importantly the on-site approximation does not introduce additional contributions to both forces and stress.

We have then presented a series of tests for group IV and III-V semiconductors and for  $5d$  metals. The overall structural parameters do not change with respect to standard non-relativistic LDA calculations, and are in general good agreement with reference data. The spin-orbit splittings of the band structures are also in good agreement with those obtained with more computationally intensive DFT methods.

The good results obtained for the electronic structures and structural parameters make our method very attractive for large scale simulations where spin-orbit coupling is relevant. This is for instance the case of semiconductors heterostructures and quantum-transport calculations<sup>29</sup> where spin-mixing effects are important.

## Acknowledgments

We wish to thank D. Sánchez-Portal, P. Ordejón and J. Soler for useful discussions. LFS acknowledges the support of FICYT through grant BP04-087. The research presented in this article has been performed under the financial support of Science Foundation of Ireland (SFI02/IN1/I175) and MEC through projects BFM2003-03156. Traveling has been supported by Enterprise Ireland (IC 2004 84).

\* Electronic address: \* m.a.oliveira@tcd.ie

<sup>1</sup> J. M. Soler, E. Artacho, J. D. Gale, A. G. J. Junquera, P. Ordejón, and D. Sánchez-Portal, *J. of Phys. C: Condens. Matter* **14**, 2745 (2002).

<sup>2</sup> H. Hohenberg and W. Kohn, *Phys. Rev.* **136**, B864 (1964).

<sup>3</sup> W. Kohn and L. Sham, *Phys. Rev.* **140**, A1133 (1965).

<sup>4</sup> S. A. Wolf, D. D. Awschalom, R. Buhrman, J. M. Daughton, S. von Molnar, M. L. Roukes, A. Y. Chtchelkanova, and D. M. Treger, *Science* **282**, 1488 (2001).

<sup>5</sup> J. M. Kikkawa and D. D. Awschalom, *Nature* **397**, 139 (1999).

<sup>6</sup> S. Sanvito, G. Theurich, and N. Hill, *Journal of Supercon-*

*ductivity and Novel Magnetic Materials* **15**, 85 (2002).

<sup>7</sup> P. Bruno, *Electronic Structure: Basic Theory and Practical Methods* (Cambridge University Press, Cambridge, 2004).

<sup>8</sup> T. Burkert, O. Eriksson, P. James, S. Simak, B. Johansson, and L. Nordstrom, *Physical Review B* **69**, 104426 (2004).

<sup>9</sup> L. M. Sandratskii, *Adv. Phys.* **47**, 91 (1988).

<sup>10</sup> V. M. García-Suárez, C. M. Newman, C. J. Lambert, J. M. Pruneda, and J. Ferrer, *Journal of Physics: Condensed Matter* **16**, 5453 (2004).

<sup>11</sup> L. Kleinman, *Phys. Rev. B* **21**, 2630 (1980).

<sup>12</sup> G. B. Bachelet and M. Schüter, *Phys. Rev. B* **25**, 2103 (1982).

- <sup>13</sup> F. Schwabl, *Quantum Mechanics* (Springer, Berlin, 2002).
- <sup>14</sup> Atomic units are used throughout the article.
- <sup>15</sup> O. Sankey and D. Niklewski, Phys. Rev. B **40**, 3979 (1989).
- <sup>16</sup> L. Kleinman and D. M. Bylander, Phys. Rev. Lett. **48**, 1425 (1982).
- <sup>17</sup> R. P. Feynman, Phys. Rev. **56**, 340 (1939).
- <sup>18</sup> G. G. Wepfer, T. C. Collins, and R. N. Euwema, Phys. Rev. B **4**, 1296 (1971).
- <sup>19</sup> J. Junquera, D. S.-P. Óscar Paz, and E. Artacho, Phys. Rev. B **64**, 1 (2001).
- <sup>20</sup> E. Anglada, J. M. Soler, J. Junquera, and E. Artacho, Phys. Rev. B **66**, 1 (2002).
- <sup>21</sup> M. P. Surh, M.-F. Li, and S. G. Louie, Phys. Rev. B **43**, 4286 (1991).
- <sup>22</sup> C. Filippi, D. J. Singh, and C. J. Umrigar, Phys. Rev. B **50**, 14947 (1994).
- <sup>23</sup> C. Kittel, *Introduction to Solid State Physics* (Wiley, New York, 1986).
- <sup>24</sup> D. E. Aspnes, Phys. Rev. B **12**, 2297 (1975).
- <sup>25</sup> K. A. Mäder and A. Zunger, Phys. Rev. B **50**, 17393 (1994).
- <sup>26</sup> A. D. Corso and A. M. Conte, Phys. Rev. B **71**, 115106 (2005).
- <sup>27</sup> V. Theileis and H. Bross, Phys. Rev. B **62**, 13338 (2000).
- <sup>28</sup> S. B. der Kellen and A. J. Freeman, Phys. Rev. B **54**, 11187 (1996).
- <sup>29</sup> A. R. Rocha, V. M. G. Suárez, S. W. Bailey, C. J. Lambert, J. Ferrer, and S. Sanvito, Nature Materials **4**, 335 (2005).